

## SYNTHESIS AND CHARACTERIZATION OF MESOPOROUS SILICA MCM-41 FROM AN INDUSTRIAL WASTE.

Shubhangi Atkare<sup>1</sup>, Dr. N. A. Kedar<sup>2</sup> and Dr. Manish Deshpande<sup>2</sup>

<sup>1</sup>Dept. of Chemistry Dayanand Science College, Latur .

<sup>2</sup>Dept. of Physics, Netaji Subhashchandra Bose College, Nanded .

### ABSTRACT :

Coal fly ash was used to synthesize MCM-41 by alkali fusion followed by hydro-thermal treatment and was characterized using various techniques viz. XRD, SEM, FTIR, BET method for surface area measurement etc. The synthesis conditions were optimized to obtain highly crystalline MCM-41 with utmost BET surface area 1102m<sup>2</sup>/g with high purity. The crystalline nature of the prepared MCM-41 was found to change with fusion temperature and a maximum value was obtained at 550<sup>0</sup> C. The cost of synthesized MCM-41 was projected to be very few as compared to that of commercial MCM-41.

**KEY WORDS :** CFA; MCM-41; X-RD; SEM.

### INTRODUCTION

The quantity of coal fly ash (CFA) generated by coal-based thermal power plants has been escalating at a shocking rate throughout the world. In India, more than 100 million tons of CFA is being generated annually with more than 75,000 acres of land being occupied by ash ponds. The disposal of such a huge amount of ash has become a pressing issue.

Several approaches have been made for the proper utilization of CFA, one of them is the conversion of CFA into mesoporous MCM-41, which have wide applications in ion exchange, as molecular sieves, catalysts, and adsorbents. In recent times, a significant concentration is given on the mesoporous catalytic materials for ensuring fast synthesis of multipurpose organic compounds owing to their high surface area, large pore size and volume. Mesoporous materials have become an alternative source to make chemical process green and environmentally benevolent. Mesoporous molecular sieves designated as M41S have attracted much attention of many researchers, since their discovery at Mobile Oil Corporation in 1992. Mesoporous MCM-41 material can be synthesized using various silica precursors.

The present study is concerned with the synthesis of MCM-41 from CFA and its characterization using various techniques. CFA is mainly composed of some oxides resulting from inorganic compounds, which remain even after the combustion of the coal. SiO<sub>2</sub> and Al<sub>2</sub>O<sub>3</sub>, are the significant contents of CFA and show few variations with the type of coal. MCM-41

synthesis processes engross the addition of Sodium Hydroxide (NaOH ) to the CFA slurry at higher temperatures. Blend of the NaOH–CFA mixture facilitates the formation of highly active Sodium-aluminate and silicates, which are eagerly soluble in water and enhance formation of MCM-41.

The synthesis of MCM-41 was also studied with CFA of varying chemical composition. Investigated effects of the hydrothermal reaction parameters such as temperatures, Molarity of NaOH and reaction time on the properties of the treated CFA and also optimized the reaction parameters to obtain best quality product. Higher pH of the solution also showed better synthesis efficiency of MCM-41. It was thought desirable to collect CFA from thermal power plant at Parali TPS Maharashtra, India and renovate it into value added mesoporous material MCM-41 which could be used as catalysts for some industrially important reactions.

## 2. EXPERIMENTAL:

### A) Materials:

The CFA sample was collected from Parali TPS, Sodium hydroxide and cetyl–tri-methyl-ammonium-bromide was procured from Sigma Aldrich Laboratories (India). Table:1 presents the physico-chemical properties of the CFA samples used in the present investigation resembles that  $\text{SiO}_2$ ,  $\text{Al}_2\text{O}_3$  and  $\text{Fe}_2\text{O}_3$  are the major constituents.

**Table-1 : Chemical Composition Of As Collected CFA**

Sr.No.	Compound	CFA Parali TPS (wt%)
1	$\text{SiO}_2$	65.12
2	$\text{Al}_2\text{O}_3$	19.87
3.	$\text{Fe}_2\text{O}_3$	6.01
4.	$\text{CaO}$	3.08
5.	$\text{K}_2\text{O}$	1.12
6.	$\text{TiO}_2$	1.71
7.	$\text{Na}_2\text{O}$	0.39
8.	$\text{MgO}$	0.81
9.	Surface area	1.48( $\text{m}^2/\text{g}$ )

### B) Synthesis of MCM-41

Initially, CFA was screened through a BSS Tyler sieve of 80-mesh size to eradicate the larger particles. The unburnt carbon along with other volatile materials present in CFA were removed by calcination at  $800^\circ\text{C}$  for 3Hr. CFA was then treated with hydrochloric acid for dealumination to remove iron to a certain extent, thereby increasing the activity, thermal stability and acidity of the synthesized material all aiming for better catalytic applications. An amorphous  $\text{SiO}_2$  component in the CFA was used as Si-source for the synthesis of MCM-41. The synthesis was carried out as follows:

30gm CFA fused with 2M NaOH solution at  $100^\circ\text{C}$  for 4 hrs under stirring condition (300 rpm) in stirred autoclave. The mixture was filtered after cooling. Further 90ml of obtained supernatant solution was mixed with 1.1 gm of cetyl tri-methyl-ammonium-bromide(CTAB) and kept under stirring (300 rpm) at  $85^\circ\text{C}$ .

After 30min, 3ml Ethyl acetate as a mild acid hydrolyser was vigorously mixed and the solution kept under stirring at 600 rpm for next 30min. The obtained solution was then allowed to cool to room temperature by natural convection and was adjusted to the selected pH by adding 5.25N

H<sub>2</sub>SO<sub>4</sub> solution under slow stirring. Precipitate obtained during pH adjustment was kept at room temperature for 18 hrs. The solid obtained after filtration was frequently washed by deionized water and dried at 100<sup>0</sup>C for 2 hrs. This dried material was calcined under air from 500<sup>0</sup>C to 800<sup>0</sup>C at the interval of 50<sup>0</sup>C at a heating rate of 1<sup>0</sup>C/min.

### 3) CHARACTERIZATION:

1. pH values were measured with a digital pH meter.
2. X-ray diffraction patterns of the collected CFA and synthesized materials were recorded on a Cu/30 kV/15 mA MiniFlex2 goniometer with a wave length of 1.540 Å.
3. Infrared (FT-IR) spectra of collected CFA and synthesized materials were recorded on a FT-IR spectrometer (ATR eco ZnSe) using dry KBr as standard reference in the range of 500-4000 cm<sup>-1</sup>.
4. Specific BET surface area was calculated using Surface area Analyzer Model SAA-2000 for all synthesized samples.

#### A) X-ray diffraction:

X-ray diffraction patterns of the collected CFA and synthesized materials were recorded on a Cu/30 kV/15 mA MiniFlex2 goniometer with a wave length of 1.540 Å. The samples were scanned from 2–10° (2θ, where θ is the angle of diffraction). Quantitative measure of the crystallinity of the synthesized MCM-41 was made by using the summed heights of major peaks in the X-ray diffraction pattern. The major peaks were selected specifically because they are slightly affected by the degree of hydration. The % crystallinity was obtained by the following relation.

$$\% \text{ Crystallinity} = \frac{\text{sum of the peak heights of unknown material} \times 100}{\text{sum of peak heights of standard material}}$$

#### B) Morphological analysis by scanning electron microscope (SEM):

The morphological structure of the raw CFA, treated CFA and synthesized MCM-41 mesoporous materials were obtained by using scanning electron micrograph. The bulk elemental composition was also estimated from SEM/EDXS by indirect method, and from these data the percentages of oxides were calculated.

#### C) Particle size and surface area:

The average particle sizes of various samples were determined by particle size analyzer. BET method was used to measure specific surface area of the samples (Surface area Analyzer Model SAA-2000).

#### D) Fourier transform infrared (FT- IR) spectra:

Infrared spectroscopic analysis of different materials was carried out to study their structural features and acidity. Infrared spectroscopic analysis of the prepared MCM-41 samples was performed with by a FT-IR spectrometer (ATR eco ZnSe) using dry KBr as standard reference in the range of 500-4000 cm<sup>-1</sup>.

## 4. RESULTS AND DISCUSSION:

### A) Mineralogical properties

The CFA mainly contains  $\text{SiO}_2$ ,  $\text{Al}_2\text{O}_3$ , traces of  $\text{Fe}_2\text{O}_3$  and the oxides of Mg, Ca, P, Ti etc. The percentage of chemical composition of CFA sample used in the current study is given in table 1. The X-ray diffraction patterns of treated CFA (using instrument Cu/30 kV/15 mA MiniFlex2 goniometer with a wave length of  $1.540 \text{ \AA}$ ) is shown in figure 1.

The XRD pattern of original fly ash mainly represents the presence of crystalline quartz and mullite and also amorphous material. CFA after treatment gives several sharp diffraction peaks, which are different from those present in the untreated CFA.

The diffractograms shows that the original crystalline phases of CFA, quartz and mullite, are mostly absent in the treated materials.

### B) Study Of Synthesized Material :

The X-ray pattern of the synthesized mesoporous silica material is an highly periodic silica phases which is normally reflected by the distinct XRD signatures at low  $2\theta$  angles from  $2^\circ$  to  $10^\circ$  as shown in Fig.2 Sharp signal in XRD spectra indicates the presence of long range order of uniform hexagonal phase in the mesoporous materials. The well defined reflections from [100] plane are a prime characteristics of the hexagonal lattice symmetry of the MCM-41 structure.

Fig1. X-RD Pattern of treated CFA:

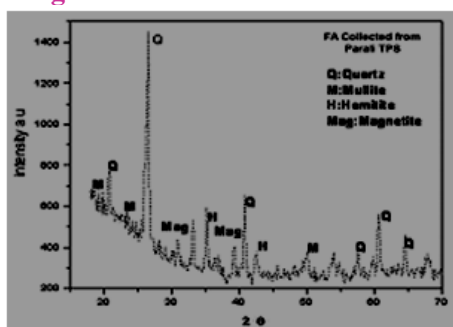
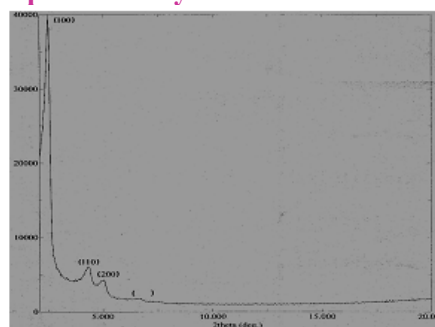


Fig2. XRD pattern of synthesized material



$d_{100}$  value =  $35.3099$ ,  $2\theta = 2.500$ , Unit cell parameter  $a_0 = \frac{2}{\sqrt{3}}d_{100}$   $a_0 = 40.8$  Intensity:  $14163$ , cps  $I/I_0 = 100$ .

The observation of three higher angle reflections other than  $d_{100}$  indicates that the product is likely to possess the symmetrical hexagonal pore structure typical of MCM-41. X-ray diffraction data therefore indicates that the supernatant of the CFA can be successfully used in the synthesis gel to prepare mesoporous materials.

### C) Structural features from infrared spectroscopy:

Even though X-ray powder diffraction data and adsorption measurements are the widely used techniques for identification of Si-MCM-41 structure, other techniques also give useful structural information as well. Infrared (IR) spectroscopy can capitulate information concerning structural details of the material. The IR spectra of the original fly ash and treated fly ash are shown in figure 4. The two most intense bands for micro-mesoporous materials usually occur at  $860\text{--}1230 \text{ cm}^{-1}$  and  $420\text{--}500 \text{ cm}^{-1}$ , which are shown more clearly in figure 3. The first is assigned to an asymmetric stretching mode and the second one to a bending mode of the T-O bond. All these bands are more or less dependent on the crystal structure. The mid infrared region of the spectrum contains the fundamental framework vibration of  $\text{Si}(\text{Al})\text{O}_4$  groupings. The IR spectral data for the absorbance band in between the wave numbers  $980\text{--}1320 \text{ cm}^{-1}$  in the IR spectrum of CFA and treated CFA

represents the presence of substituted Al atoms in the tetrahedral forms of silica frameworks. All these observations confirm the formation of MCM-41 on alkali and hydrothermal treatments of CFA.

**Fig.3 FT-IR of calcined CFA**

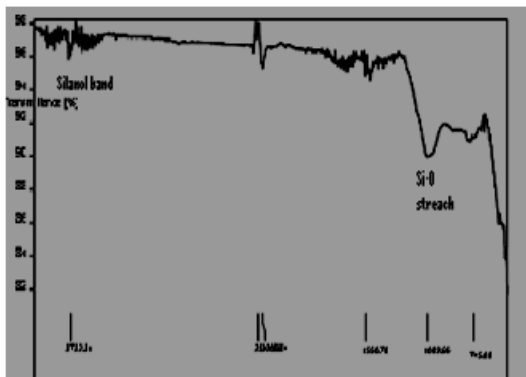


**Fig.4 FT-IR of synthesized material**

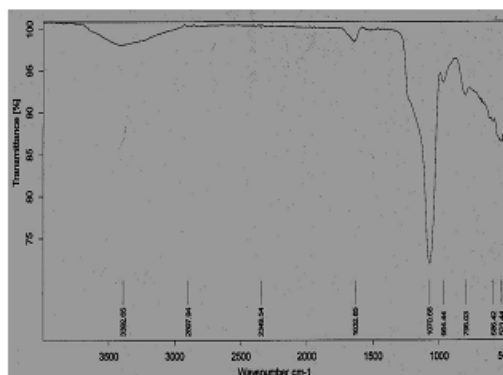


**Table 2. Zeolite IR assignments.**

Internal tetrahedral: Asymmetric stretch 1250–950 Symmetric stretch 720–650 T–O bend 420–500

External linkage: Double ring 650–500 Pore opening 300–420 Symmetric stretch 750–820 Asymmetric stretch 1050–1150

The FT-IR spectra of as synthesized Si-MCM-41 from coal fly ash are shown in Fig.4 From FT-IR spectra, the absorption bands around 2921 and 2851  $\text{cm}^{-1}$  correspond to n-C-H and d-C-H vibrations of the surfactant molecules, such bands disappeared in the calcined sample indicating the total removal of organic material during calcinations. The broad band around 3392.65  $\text{cm}^{-1}$  as observed due to surface silanols and O-H stretching frequency of adsorbed water molecule. Moreover the peaks in the range of 1500-1600  $\text{cm}^{-1}$  are because of the deformation mode of surface hydroxyl group. A peak at 1070.63  $\text{cm}^{-1}$  and 964.44  $\text{cm}^{-1}$  corresponds to the asymmetric and symmetric Si-O groups, respectively. The peaks in the range 1010-1079  $\text{cm}^{-1}$  are assigned to M-O-M bonding, the bands from 960 to 990  $\text{cm}^{-1}$  appeared due to Si-O-M (M=metal ions) vibrations in metal incorporated silanols.

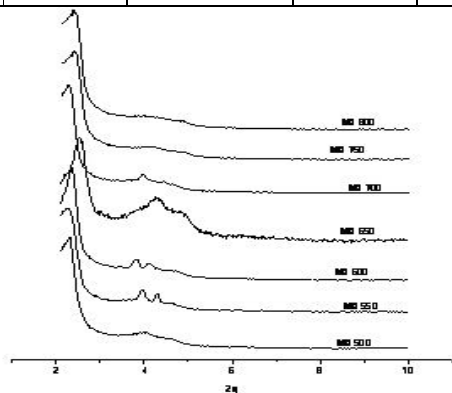
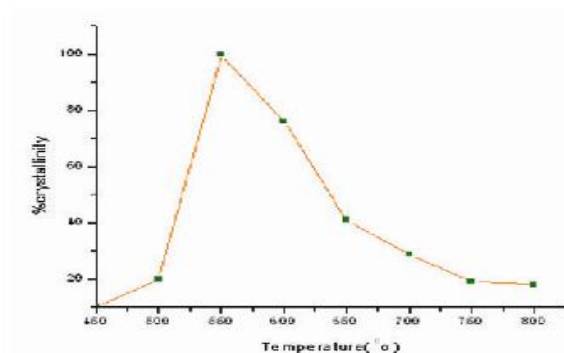
#### **D) Study of the effect of various parameters:**

##### **1. Effect of change of Calcination temperature when pH=6.91 & Duration 4 Hrs**

The effect of change of calcinations temperature shows that, at 550 $^{\circ}\text{C}$  keeping pH of the gel 6.91 and calcinations duration of 4 hrs, the Synthesized material was found to be more crystalline. The crystallinity reduces below and above 550 $^{\circ}\text{C}$ . The X-RD patterns and variation of calcinations temperature with % crystallinity is as shown in fig.5 and fig.6

**Table 3: The effect of change calcination temperature**

Sr. No .	Sample Name	Calcination temp.	2 $\theta$ for d <sub>100</sub>	d <sub>100</sub>	Intensity	a <sub>0</sub>	% Crystallinity	BET Surface Area
1.	MDT <sub>1</sub>	500 <sup>0</sup> C	2.32	38.04	3412	44.1 0	20	976.653
2.	MDT <sub>2</sub>	550 <sup>0</sup> C	2.50	35.30	14163	40.9 0	100	1101.788
3.	MDT <sub>3</sub>	600 <sup>0</sup> C	2.46	38.19	3767	44.3 0	76	---
4.	MDT <sub>4</sub>	650 <sup>0</sup> C	2.54	34.75	1574	40.3 1	41	---
5.	MDT <sub>5</sub>	700 <sup>0</sup> C	2.38	37.08	4979	43.0 2	29	801.316
6.	MDT <sub>6</sub>	750 <sup>0</sup> C	2.42	36.47	4801	42.3 1	19	---
7.	MDT <sub>7</sub>	800 <sup>0</sup> C	2.41	36.17	4713	41.9 0	18	767.130

**Fig.5 XRD patterns of sample at different calcination temperature****Fig.6 Relation Between % crystallinity with Temperature**

## 2. Effect of change of Calcination time when pH=6.91 & Calcination temp. 550<sup>0</sup>C

**Table 4 : The effect of change calcination duration**

Sr. No .	Sample Name	Calcination temp.	2 $\theta$ for d <sub>100</sub>	d <sub>100</sub>	Intensity	a <sub>0</sub>	% Crystallinity	BET Surface Area
1.	MDH <sub>1</sub>	01.30	2.38	37.08	7136	43.0 0	76	386.184
2.	MDH <sub>2</sub>	03.00	2.46	35.88	3599	41.6 0	99	----
3.	MDH <sub>3</sub>	04.30	2.50	35.30	14163	40.9 0	100	1101.788
4.	MDH <sub>4</sub>	06.00	2.32	38.04	5202	44.1	89	----

						0		
5.	MDH <sub>5</sub>	07.30	2.32	38.04	5166	44.1	75	620.702
						0		
6.	MDH <sub>6</sub>	12.00	4.10	21.53	952	25.0	61	564.092
						0		

The effect of change of calcinations time duration shows that, for 4 hrs, keeping pH of the gel 6.91 and calcinations temperature 550<sup>0</sup>C the synthesized material was found to be more crystalline. The crystallinity reduces for calcinations timings less than 4 hrs and greater than 4 hrs. The X-RD patterns and variation of calcinations time with % crystallinity is as shown in fig.7 and fig.8

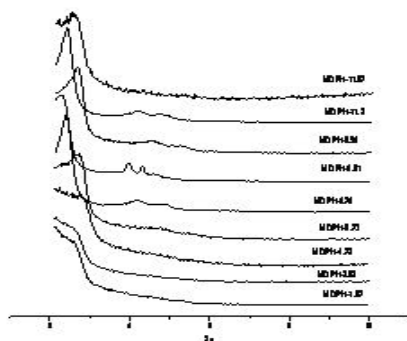


Fig. 7 XRD patterns of sample at different calcination durations

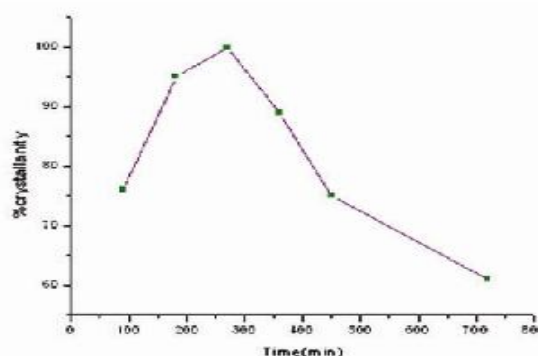


Fig.8 Relation Between % crystallinity with Time variation

### 3). Effect of change of pH of gel at Calcination temp.550<sup>0</sup>C for 4hrs.

Table 5 : Effect of pH Variation

Sr. No .	Sample Name	Calcination temp.	2θ for d <sub>100</sub>	d <sub>100</sub>	Intensity	a <sub>0</sub>	% Crystallinity	BET Surface Area
1.	MDP <sub>1</sub>	1.87	2.64	33.43	1155	38.8	19	632.161
2.	MDP <sub>2</sub>	3.82	2.66	33.18	899	38.5	28	---
3.	MDP <sub>3</sub>	4.72	2.86	30.86	820	35.8	37	---
4.	MDP <sub>4</sub>	5.73	2.28	38.71	767	44.9	38	976.181
5.	MDP <sub>5</sub>	6.76	2.39	35.91	4103	41.7	84	----
6.	MDP <sub>6</sub>	6.91	2.50	33.30	14163	40.9	100	1101.788
7.	MDP <sub>7</sub>	8.56	2.68	32.93	3359	38.2	59	682.871
8.	MDP <sub>8</sub>	11.2	2.40	36.78	5793	42.7	28	368.121
9.	MDP <sub>9</sub>	11.87	2.60	33.95	657	39.4	25	14.274

The effect of change of pH of gel shows that, for calcinations temperature 550<sup>0</sup>C for 4 hrs. the synthesized material was found to be more crystalline. The crystallinity reduces when pH of the gel is below 6.91 and above 6.91. As observed in the effect of change in the initial pH value, the XRD data suggests that the pH of gel plays an important role in the formation of MCM-41. The hexagonal unit cell parameter a<sub>0</sub> in the calcined sample increased with synthesis pH value. The variation of pH of gel with % crystallinity is as shown in fig. 9

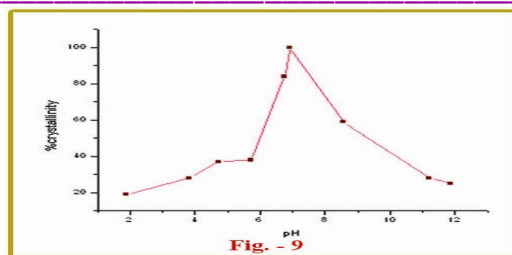


**Fig.9 Relation Between % crystallinity with pH of gel solution**

### E. N<sub>2</sub>-Adsorption Desorption Analysis of Synthesized Material :

Nitrogen physisorption probes the textural properties of materials i.e. surface area, pore volume, pore size and pore geometry. At very low relative pressures ( $p/p_0$ ) a very large amount of nitrogen becomes physisorbed which assigns to condensation of nitrogen inside and outside on the surface of MCM-41.

As the surface area is very high this corresponds monolayer adsorption. Upon monolayer adsorption multilayer of nitrogen starts to developed at higher relative pressures. Also in this case both the external surface area and mesopores contributes to the physisorption process. The collected data from the N<sub>2</sub> adsorption desorption graph is used to calculate the surface area of the material using BET method. (Tables 3, 4 & 5)

From Table 3 it is seen that as calcination temperature of synthesized sample changes keeping pH of gel and duration invariant, initially % crystallinity increases and then reduces. Similarly the specific surface area also varies in the same fashion.

From table 4 it is observed that the calcination duration affects prominently on specific surface area of a synthesized sample. i.e.for smaller duration, it is less. After a particular range of duration i.e. about 4.30 hrs. It again reduces accordingly.

From table 5 it can be summarized that, for lower pH of gel the specific surface area is considerably small and increases as the pH of gel increases. Beyond a particular pH i.e. above 6.91, surface area again decreases in sequence.

From the above tabular data it is confirmed that the maximum calculated surface area amounts to 1102m<sup>2</sup>/g. for the Si-MCM-41 materials keeping pH of gel 6.91, calcination time 4.30 hrs.at 550<sup>0</sup>C.

### F) Scanning Electron Micrograph Study

**Fig:10 The SEM micrographs of the original CFA**

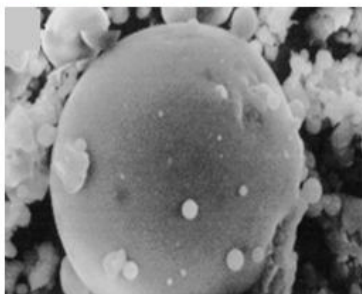


**Fig:11 The SEM micrographs of the treated CFA**

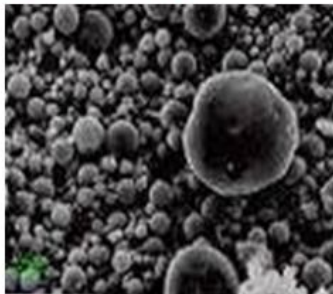
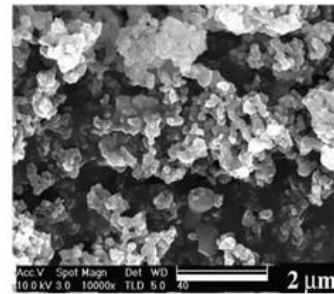


**Fig: 12 The SEM micrographs of the synthesized Si-MCM-41**



The scanning electron micrographs (SEM) of the original CFA figure 11, treated CFA figure 12 and synthesized Si-MCM-41 figure 10 are shown. The absence of the spherical particles in treated CFA indicates its high conversion into crystalline Si-MCM-41 on hydrothermal treatment. The crystal structure of the synthesized material was determined to be well ordered regular hexagonal.

### CONCLUSIONS:

Based upon the experimental study it was concluded that pure and ordered Si-MCM-41 material could be successfully synthesized from coal fly ash at room temperature during 18 hrs of reaction. The parametric variations such as change of calcination temperature, the change of calcination time duration and the change of initial pH value of gel suggested that from CFA the well ordered mesoporous material Si-MCM-41 can be synthesized at 550°C for 4.30 hrs keeping pH of gel 6.91. This study demonstrates that converting CFA into mesoporous materials not only eliminates the disposal problem of CFA but also turns a waste material into a useful one. The synthesized Si-MCM-41 materials may find applications in the waste water treatment, Chemical industries and Agriculture industry etc. The proposed method provides one of the ways of recycling CFA.

### REFERENCES:

1. J.S. Beck, J.C. Vartuli, W.J. Roth, M.E. Leonowicz, C.T. Kresge, K.D. Schmitt, C.T.-W. Chu, D.H. Olson, E.W. Sheppard, S.B. McCullen, J.B. Higgins and J.L. Schlenker, *J. Am. Chem. Soc.*, **1992**, *114*, 10834-10843.
  2. D.H. Park, C.-F. Cheng, H. He and J. Klinowski, *J. Mater. Chem.*, **1997**, *7*(1), 159-162.
  3. K.M. Reddy, I. Moudrakovski and A. Sayari, *J. Chem. Soc., Chem. Commun.*, **1994**, 1059-1060.
  4. J.S. Reddy and A. Sayari, *J. Chem. Soc., Chem. Commun.*, **1995**, 2231-2232.
  5. T. Blasco, A. Corma, M.T. Navarro and J. Pérez Pariente, *J. Catal.*, **1995**, *156*, 65-74.
  6. M.D. Alba, Z. Luan and J. Klinowski, *J. Phys. Chem.*, **1996**, *100*(6), 2178-2182.
  7. A. Corma, M.T. Navarro and J.P. Pérez-Pariente, *J. Chem. Soc., Chem. Commun.*, **1994**, 147-148.
  8. A. Corma, M. Iglesias and F. Sánchez, *Catal. Lett.*, **1996**, *39*(3/4), 153-156.
  9. O. Franke, J. Rathousky, G. Schulz-Ekloff, J. Stárek and A. Zúkal in *Zeolites and Related Microporous Materials: State of the Art 1994.*; Stud. Surf. Sci. Catal., (Eds. J. Weitkamp, H.G. Karge, H. Pfeifer and W. Hölderich), Elsevier Science B.V., **1994**, *Vol. 84*, 77-84.
  10. S. Gontier and A. Tuel, *Zeolites*, **1995**, *15*, 601-610.
  11. P.T. Tanev, M. Chibwe and T.J. Pinnavaia, *Nature*, **1994**, *368*, 321-323.
  12. A. Tuel, S. Gontier and R. Teissier, *J. Chem. Soc., Chem. Commun.*, **1996**, 651-652.
  13. Z.Y. Yuan, S.Q. Liu, T.H. Chen, J.Z. Wang and H.X. Li, *J. Chem. Soc., Chem. Commun.*, **1995**, 973-974.
- Synthesis* 30
14. D. Zhao and D. Goldfarb, *J. Chem. Soc., Chem. Commun.*, **1995**, 875-876.
  15. N. Ulagappan and C.N.R. Rao, *J. Chem. Soc., Chem. Commun.*, **1996**, 1047-1048.
  16. M. Hartmann, A. Pöpl and L. Kevan, *J. Phys. Chem.*, **1996**, *100*(23), 9906-9910.
  17. M. Hartmann, A. Pöpl and L. Kevan, *J. Phys. Chem.*, **1995**, *99*(49), 17494-17496.
  18. T.M. Abdel-Fattah and T.J. Pinnavaia, *J. Chem. Soc., Chem. Commun.*, **1996**, 665-666.
  19. T.K. Das, K. Chaudhari, A.J. Chandwadkar and S. Sivasanker, *J. Chem. Soc., Chem. Commun.*, **1995**, 2495-2496.
  20. C.-F. Cheng, H. He, W. Zhou, J. Klinowski, J.A.S. Gonçalves and L.F. Gladden, *J. Phys. Chem.*, **1996**, *100*, 390-396.